Design and Implementation of a Floating Meminductor Emulator upon Riordan Gyrator

Francisco J. Romero[1,*], Alfredo Medina-Garcia[2], Manuel Escudero[3], Diego P. Morales[1] and Noel Rodriguez[1]

[1] Dept. Electronics and Computer Technology, Faculty of Sciences, University of Granada, 18071 Granada, Spain.

[2] Infineon Technologies AG, 85579 Neubiberg, Germany

[3] Infineon Technologies Austria AG, 9500 Villach, Austria

[*] Email: franromero@ugr.es

Abstract

In this communication we present the design, simulation and implementation of a floating flux-controlled meminductor emulator based on the Riordan gyrator. Firstly, the circuit is presented theoretically, from its original version to emulate inductors to its adaptation for floating meminductors. Once its theoretical equations are presented, using SPICE simulations, we demonstrate the feasibility of this implementation by means of off-the-shelf components and a memristor, or a memristor emulator, for different inputs signals and frequencies in both grounded and floating configurations. Finally, a low-frequency breadboard-level implementation is included to prove its practicality.

Keywords: circuit theory, emulator, feedback, gyrator, meminductor, memristor

1. Introduction

Nearly 50 years ago, Prof. Leon Chua presented for the first time the passive circuit element which established the relation between flux (ϕ, time-integral of the input-voltage) and charge (q) [1]. This element was called *memristor (memory-resistor)* since it demonstrated that, for a given voltage, its resistance at an instant $t = t_1$ depends not only on the current at t_1, but also on the current through the device from $t = -\infty$ to $t = t_1$, hence presenting a memory characteristic. However, it was not until 2008 that a group of researchers from Hewlett-Packard Labs (HP) reported the first solid-state device exhibiting memristive behavior [2]. It was then when the concept of memristor ushered in unprecedented electronic devices and applications, extending from ReRAMs (Resistive Random-Access Memory) to realistic neural networks [3]. Thus, the memristor, and its non-volatile memory effect, has raised as one of the more substantial revolutions in the field of electronic circuits theory since the invention of the transistor [4].

In 2009, after the great interest aroused by memristive devices, M. Di Ventra, Y.V. Pershin and L. Chua generalized the concept of memory devices to capacitors and inductors, thus defining the *memcapacitor* and the *meminductor* [5]. In these devices, both capacitance and inductance, as in the case of memristors, present a non-volatile memory effect which depends not only on its present state but also on the history of the device. In this way, apart from the definition of memristor (R_M, Eq.1), they defined the concepts of memcapacitor (C_M, Eq. 2), as the nth-order system that establishes a nonlinear relation between the charge (q) of the device and its voltage (V); and the meminductor (L_M, Eq. 3), as the nth-order system which establishes the nonlinear relation between current (I) and flux (ϕ) [6].

$$V(t) = R_M(\overrightarrow{\boldsymbol{x_N}}, I, t) \cdot I(t) \tag{1}$$

$$q(t) = C_M(\overrightarrow{\boldsymbol{x_N}}, V, t) \cdot V(t) \tag{2}$$

$$\phi(t) = L_M(\overrightarrow{\boldsymbol{x_N}}, I, t) \cdot I(t) \tag{3}$$

Being $\overrightarrow{\boldsymbol{x_N}}$ a vector representing the *n* internal state variables of the system.

These devices, memcapacitor and meminductor, are expected to cause a disruption in the field of electronics, which has led to several studies on diverse applications, such as neuromorphic and quantum computation [7], [8], logic gates [9], [10], self-adaptative filters [11]–[13] or chaotic circuits [14]–[18]. However, in contrast to memristors, which can be already fabricated relying on different materials and resistive switching mechanisms [2], [19]–[21], solid-state memcapacitors and meminductors are yet elusive.

For this reason, in recent years many SPICE models as well as some practical implementations of memcapacitors and meminductors emulators have been proposed. These circuits follow different alternatives to achieve the same goal: satisfying the constitutive equations of the emulated device. These alternatives can be grouped into two main groups; *i)* those using another mem-device (in particular a memristor) to mutate its behavior to the desired mem-device and *ii)* those not based on mem-devices. Thus, many of the different memcapacitors and meminductors emulators use a memristor (or a memristor emulator) to transform its constitutive equations into the constitutive relation of the mem-device emulated [22]–[28], as it is done in this work, while the rest of them make use of classical voltage-mode op-amps (VOAs), current feedback operational amplifiers (CFOAs), operational transconductance amplifier (OTAs) and/or current conveyors to emulate the desired mem-device [14], [29]–[36].

However, the implementation of most of these circuits limits the emulated device to grounded configurations, hence reducing their potential applications. In order to avoid this, in this work we present a simple and low-cost floating meminductor emulator based on a modification of the Riordan gyrator, typically used to emulate floating inductors and whose design is based on classical op-amps [37].

The manuscript is structured as follows: after this introduction, Section 2 presents the theoretical modifications over the Riordan gyrator to achieve a meminductive behavior, together with SPICE simulations demonstrating the feasibility of the proposed circuit for floating and grounded configurations. After that, a simple low-frequency breadboard-level implementation using off-the-shelf components is presented in Section 3 and, finally, the main conclusions are drawn in Section 4.

2. Meminductance and the modified Riordan gyrator.

As defined by Chua [6], the meminductive systems can be either current-controlled or flux-controlled depending on the relation of the meminductance with these parameters. This work is focused on flux-controlled meminductive systems, which are described by the following equations:

$$I(t) = L_M^{-1}(x_1, x_2, \dots, x_n, \phi, t) \cdot \phi(t) \tag{4}$$

$$\frac{d\overrightarrow{\boldsymbol{x_N}}}{dt} = f(\overrightarrow{\boldsymbol{x_N}}, \phi, t) \tag{5}$$

being t the time, $\overrightarrow{\boldsymbol{x_N}}$ the N-component vector defining the N state variables of the system and f a continuous n^{th}-dimensional vector function.

A particular case of this general definition is the flux-controlled meminductor, a meminductive system with one single state variable whose meminductance depends only on the input flux. In that case, Eq. 4 and Eq. 5 can be reduced to Eq. 6 [6]:

$$I(t) = L_M^{-1}\left[\int_{t_0}^{t}\phi(\tau)d\tau\right]\cdot\phi(t) \tag{6}$$

provided that $\int_{-\infty}^{t_0}\phi(\tau)d\tau = 0$. Note that a flux-controlled meminductor is not only an inductor whose inductance depends on the time integral of the input flux, but also whose current–flux characteristic presents a pinched hysteresis loop (in which the current is zero whenever the flux is zero) [6].

On this basis, here we demonstrate that the Riordan gyrator [37], after certain modifications (see Figure 1), is suitable for the emulation of floating flux-controlled meminductors.

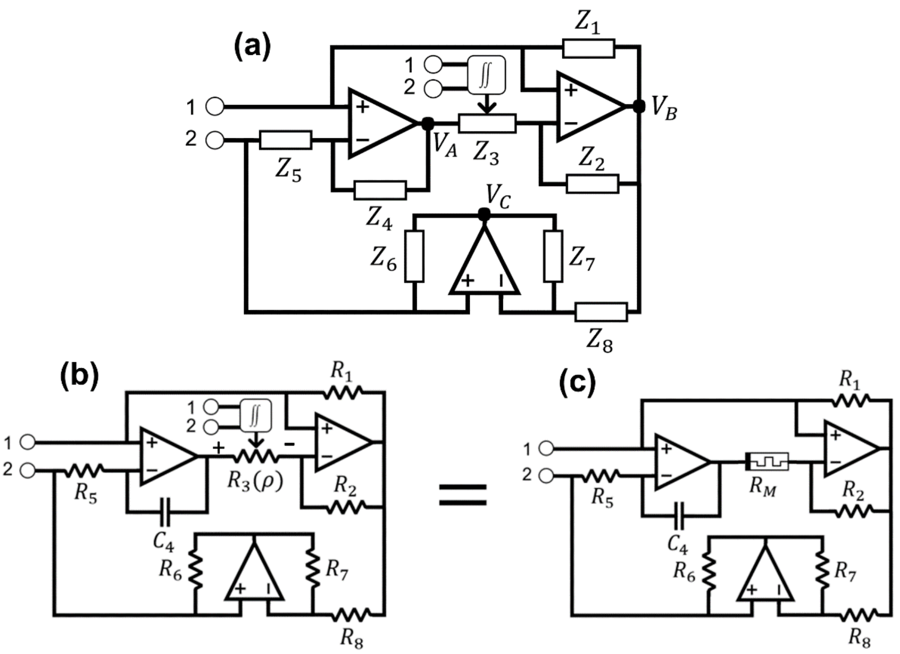

Figure 1. (a) Modified Riordan gyrator using an impedance *Z₃* whose value depends on the double time integral of the input voltage. (b) Adaptation of the circuit shown in (a) to emulate flux-controlled meminductors. (c) Circuit equivalent to the one shown in (b).

Firstly, for a floating impedance, the input current at terminal one must be equal to the output current of terminal two:

$$I_1 = -I_2 \tag{7}$$

Neglecting the input bias current of the op amps, the input current at terminal one corresponds to the current through the impedance Z_1, and therefore, it can be obtained as indicated in Eq. 8.

$$I_1 = \frac{V_{IN_1} - V_B}{Z_1} = \left(V_{IN_1} - V_{IN_2}\right) \cdot \frac{Z_2 Z_4}{Z_5 Z_3 Z_1} = V_{IN} \cdot \frac{Z_2 Z_4}{Z_5 Z_3 Z_1} \tag{8}$$

In the same way, the current at terminal two corresponds to the sum of the current through Z_6 and Z_5, which can be derived as expressed in Eq. 9.

$$I_2 = \frac{V_{IN_2} - V_{IN_1}}{Z_5} + \frac{V_{IN_2} - V_C}{Z_6} = V_{IN} \cdot \left(\frac{Z_7}{Z_8 Z_6} + \frac{Z_2 Z_4 Z_7}{Z_3 Z_5 Z_6 Z_8} - \frac{1}{Z_5}\right) \tag{9}$$

Thus, in order to satisfy Eq. 7, the circuit shown in Figure 1a needs to fulfill the following condition:

$$\frac{1}{Z_5} = \frac{1}{Z_1} = \frac{Z_7}{Z_6 Z_8} \tag{10}$$

In that case, and considering Z_3 as a flux-controlled impedance, the value of the lossless floating flux-controlled input impedance of the circuit can be expressed as indicated in Eq. 11 in Laplace's domain.

$$Z_{1\to 2}(\rho(s)) = \frac{Z_1 Z_3 \left(\frac{\phi(s)}{s}\right) Z_5}{Z_2 Z_4} \tag{11}$$

This impedance, after the substitutions shown in Figure 1b, can be directly related to a flux-controlled inductance (see Eq. 12) considering $R_1 = R_2 = R_5 = R_6 = R_7 = R_8 = \boldsymbol{R}$, and a resistance $R_3(\rho)$ controlled by the time integral of the flux (ρ).

$$Z_{1\to 2}(\rho(s)) = \boldsymbol{s}RC_4R_3\left(\frac{\phi(s)}{s}\right) = \boldsymbol{s}L\left(\frac{\phi(s)}{s}\right) \tag{12}$$

This also makes feasible the circuit of Figure 1b satisfies the constitutive equation of a meminductor, given that:

$$I_1 = \frac{1}{RC_4R_3\left(\frac{\phi(s)}{s}\right)} \cdot \frac{V_{IN}}{s} \rightarrow \ I_1(t) = \frac{1}{L(\rho)} \cdot \phi(t) \tag{13}$$

Moreover, if we further analyze this circuit considering close to ideal operational amplifiers, it can be derived that the voltage across $R_3(\rho)$ can be expressed as a function of the input flux (ϕ) (Eq. 14).

$$V_{R_3}(t) = \ V_{R_3^+}(t) - V_{R_3^-}(t) = \frac{1}{R_5C_4}\int \left(V_{in_1}(t) - V_{in_2}(t)\right)dt = \frac{1}{R_5C_4}\int V_{in}(t)dt = \frac{\phi(t)}{R_5C_4} \tag{14}$$

Therefore, given that the resistance $R_3(\rho)$ changes its value according to the time-integral of the input flux (ρ), it is really changing its value as a function of the time-integral of its own input, hence behaving as a voltage-controlled memristor [6]. On this basis, $R_3(\rho)$ could be replaced by a voltage-controlled memristor, as illustrated in Figure 1c, which would allow to formulate Eq. 12 in terms of memristance, as indicated in Eq. 15.

$$Z_{1\to 2}(\rho(s)) = \boldsymbol{s}RC_4R_M = \boldsymbol{s}L(\rho(s)) \tag{15}$$

To prove the feasibility of the circuit to emulate a meminductor, we have considered the simple two-states meminductor implementation depicted in Figure 2.

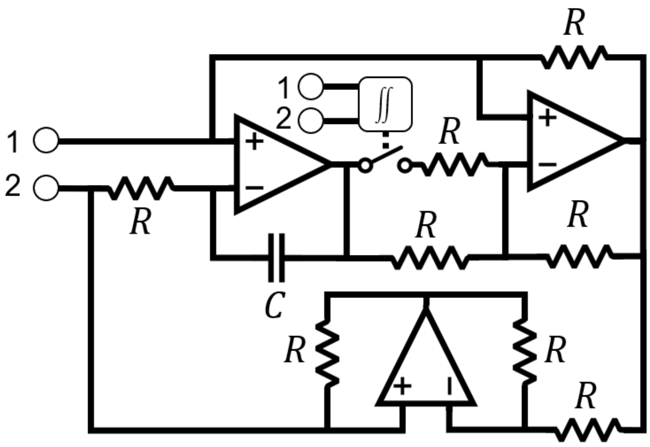

Figure 2. Two-states meminductor emulator based on the Riordan gyrator.

In the circuit of Figure 2, the value of the time integral of the input flux is obtained by integrating the input voltage twice (e.g., using differential op-amp voltage-mode integrators [39]). This value is then used to control a voltage-controlled switch that will connect (or not) the additional resistor to the feedback loop. Under this configuration, the flux-controlled inductance given in Eq. 12 can be expressed as follows:

$$L(\rho) = \begin{cases} R^2C & if\ \rho < \rho_{TH} \\ \dfrac{R^2C}{2} & if\ \rho \geq \rho_{TH} \end{cases} \quad (16)$$

where ρ_{TH} is the defined threshold value which triggers the switch.

This bistable configuration has been simulated with SPICE in order to confirm its meminductive behavior. For that, we considered the following configuration: R = 1 kΩ, C = 47 nF and ρ_{TH} = 0 V·s^2, which results in the following values of inductance according to Eq. 16: $L(\rho)$ = 47 mH for ρ < 0 and $L(\rho)$ = 23.5 mH for ρ > 0.

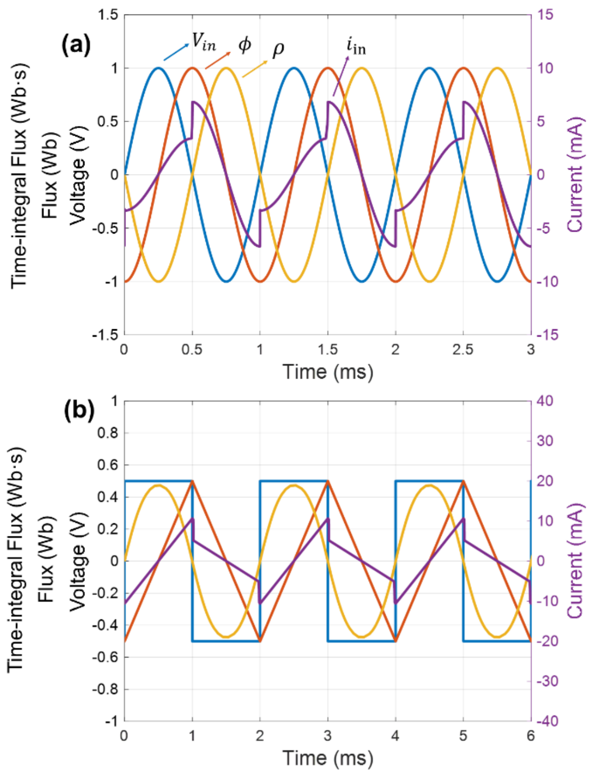

Figure 3. Simulation of the two-states meminductor emulator using a sinusoidal input signal with a frequency of 1 kHz (a) and a square input signal of 500 Hz (a).

The results shown in Figure 3 demonstrate that the circuit proposed behaves as a two-states meminductor regardless of the input signal. As seen, the emulator satisfies the constitutive equation of the meminductor (Eq. 6), since the input current is zero whenever the input flux is zero and its waveform is a function of the input flux and the state of inductance (which in turn depends on the time-integral of input flux as indicated by Eq. 16). In the same way, the meminductive behavior is also manifested in the closed pinched hysteresis loop of its *i*-ϕ characteristic (Figure 4), which has been obtained using a sinusoidal input signal with different frequencies (1 kHz and 10 kHz). In addition, the *i*-*v* characteristic of R_3 (inset of Figure 4) also proves that the voltage-controlled resistor behaves as a memristor, hence demonstrating the feasibility of the implementation shown in Figure 1c.

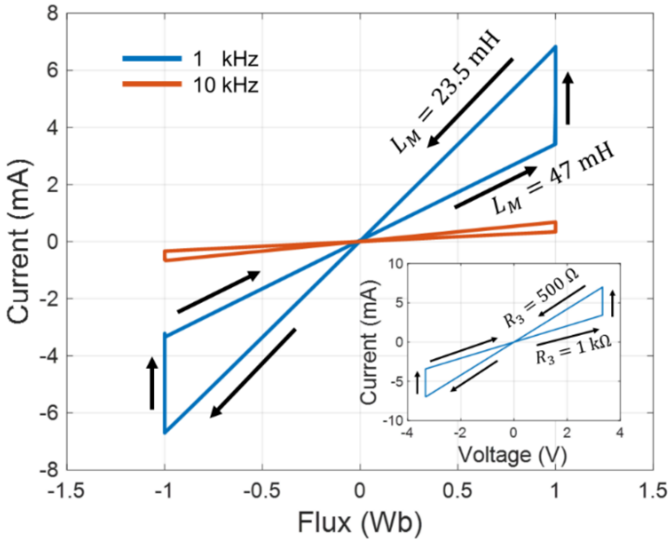

Figure 4. Closed pinched hysteresis loop of the *i*-ϕ characteristic obtained using a sinusoidal input signal at different frequencies. Inset shows the closed pinched hysteresis loop in the *i*-*v* characteristic of the voltage-controlled resistor.

3. Example in a floating configuration.

In order to probe de feasibility of the proposed meminductor emulator to be used in floating configurations, in this section we shown a simple low-pass filter based on the circuit shown in Figure 5.

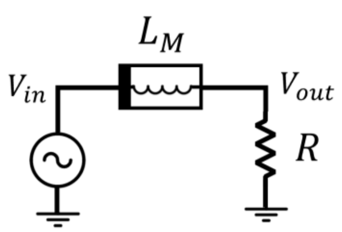

$$\omega_c = \frac{R}{L_M}$$

$$|H(j\omega)| = \frac{\omega_c}{\sqrt{\omega^2 + \omega_c^2}}$$

$$\measuredangle H(j\omega) = -\arctan\left(\frac{\omega}{\omega_c}\right)$$

Figure 5. Low-pass filter based on a meminductor and a resistor connected in series. Equations correspond to the cutoff frequency (ω_c) and the modulus ($|H(j\omega)|$) and phase ($\measuredangle H(j\omega)$) of the transfer function in the frequency domain.

For this implementation we have considered the same circuit as the one used in the previous sections but replacing the two-states memristor by a continuous states memristor (R_M) described by Eq. 17, where R_0 = 1 kΩ, and k = 500 Ω is a scale factor of the double integration of the voltage between the meminductor's terminals.

$$R_M = R_0 + \mathrm{k} \cdot \rho \tag{17}$$

The circuit was simulated using a R = 1 kΩ and an input signal with a frequency of 1 kHz, thus obtaining directly from the meminductor emulator the signals shown in Figure 6a. Note that under this configuration, the emulator also behaves as a meminductor, although in this case as a continuous-states meminductor, as the pinched hysteresis loop of Figure 6b indicates.

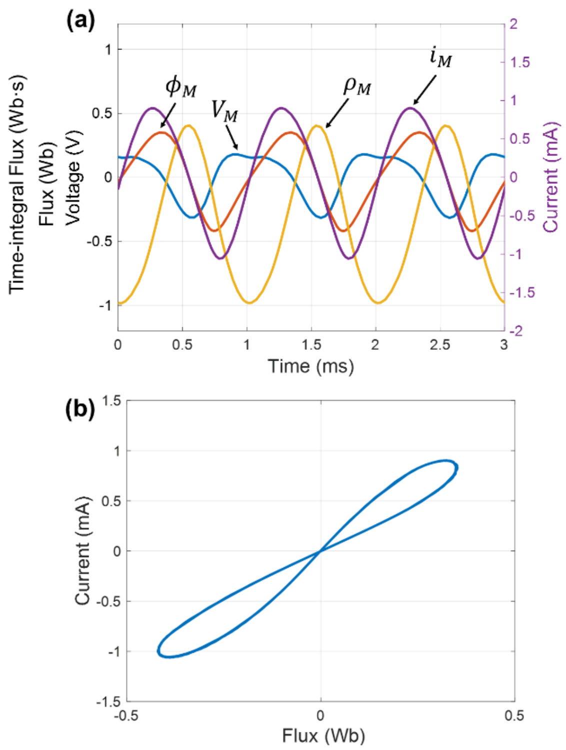

Figure 6. (a) Meminductor signals and (b) closed-pinched hysteresis loop of the i-ϕ characteristic under the low-pass filter configuration.

Therefore, according to Eq. 15 and Eq. 17, the meminductance takes continuous values in the range L_M = [24, 56.5] mH as a function of the time-integral of the input-flux (Figure 7a). The continuous change in the meminductance, in turn, makes that cut-off frequency of the low pass filter change over time (see Figure 7a), indicating that both magnitude and phase of the output signal will depend not only on the amplitude and frequency of the input signal, but also on the instantaneous value of meminductance. This effect is represented in Figure 7b, where it can be seen how the delay between both input and output signals increases as the cut-off frequency decreases.

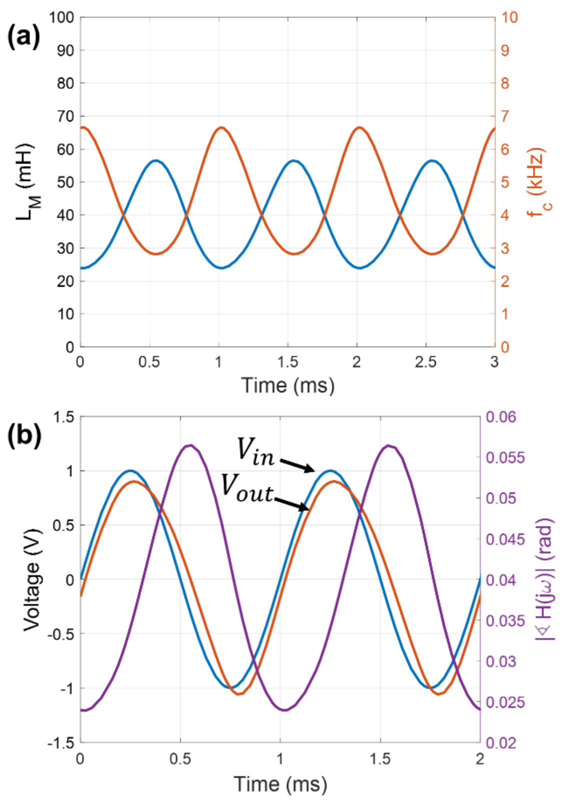

Figure 7. (a) Meminductance and cut-off frequency of the filter over time. (b) Input and output signals and delay between them over time.

4. Experimental results.

A simple breadboard-level implementation has been carried out in order to demonstrate the feasibility of this circuit by means of experimental results. For the sake of simplicity, to obtain the double time integral of the input voltage, we have considered the implementation shown in Figure 8, which allows to test the meminductor emulator for sinusoidal input signals (if the waveform of the input is of the type sin(ωt), then the waveform of its double time integral corresponds to the type -sin(ωt)).

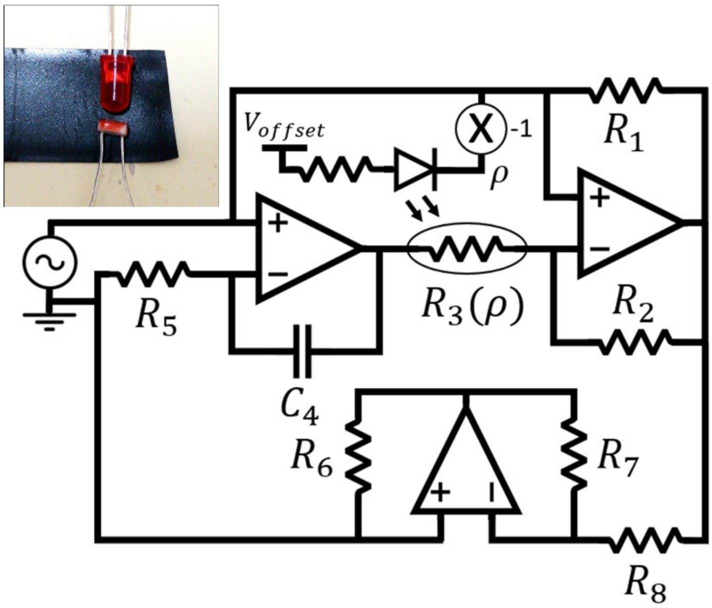

Figure 8. Meminductor emulator based on the Riordan gyrator for sinusoidal input signals. Inset shows the in-house voltage-controlled resistance used for this implementation.

In this case, the voltage-controlled resistance was implemented using a LED optically coupled to a photo resistance, as shown in the inset of Figure 8. Under this configuration, the brightness of the LED changes according to the time integral of the input flux, and therefore so does the resistance R_3. Moreover,

V_{offset} must be set to ensure that the LED never turns off, hence avoiding that the current through R_3 takes values close to zero [36], [40].

The values of the passive circuit elements were chosen as follows: $R_1 = R_2 = R_5 = R_6 = R_7 = R_8 = 10$ kΩ and $C = 47$ nF, besides, LM-741 were used to implement all op-amps configurations. A sinusoidal signal was applied to the input of the circuit with an amplitude of 50 mV and a frequency of 13 Hz (to ensure the proper response of the photoresistor), whereas V_{offset} was set to 1.8 V.

Figure 9 shows the experimental signals extracted from the meminductor emulator under the configuration previously described. In this case, the input voltage corresponds to V^{+}_{R1}, whereas V^{-}_{R1} helps to obtain the meminductor input current (neglecting the input bias current of the op-amps).

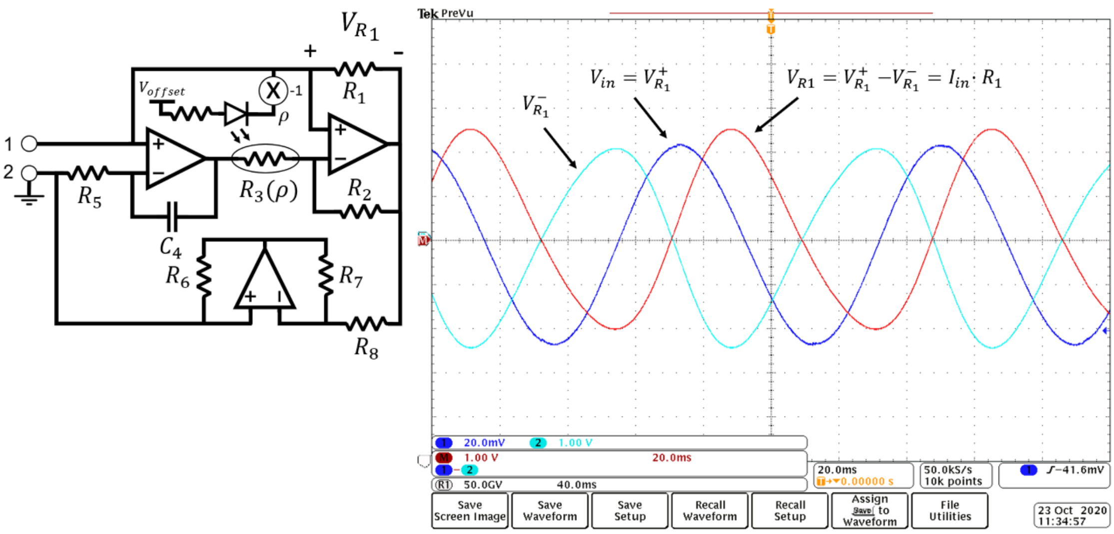

Figure 9. Experimental results of the meminductor emulator for an input signal with an amplitude of 50 mV and a frequency of 13 Hz. Signals were acquired with a Tektronix MSO 4104 mixed signal oscilloscope in high-resolution mode with a record length of 10k point (sampling rate: 50 kSamples/s).

The input flux can also be derived from the input voltage. Since this latter follows a *sin(ωt)* function, its integral waveform will correspond to the type *-cos(ωt)*, or in other words, the input flux will have a delay of *-π/2* rad with respect to the input voltage (which corresponds to a time delay of Δt = -0.02 s for the frequency used). On this basis, it is possible to plot the input current as a function of the input flux, as shown in Figure 10, demonstrating that the meminductor emulator of Figure 8 presents a continuous closed pinched hysteresis loop in its *i-ϕ* characteristic, and hence proving its meminductive behavior.

Finally, the same experiments were performed using a V_{offset} of 1.7 V instead of 1.8 V, as also shown in Figure 10. Note that in that case the current through the LED is lower than in the previous case, resulting in a lower brightness, and therefore, in higher values of R_3. Since R_3 takes higher values, so does the meminductance (see Eq. 9), which in turn produces a decrease of the input current with respect to the input flux, as defined by the constitutive equation of the meminductor (Eq. 6).

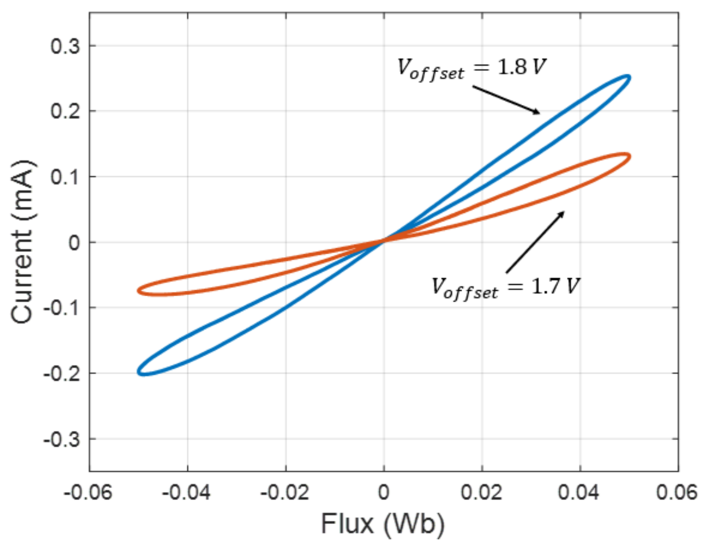

Figure 10. Experimental closed pinched hysteresis loop of the i-ϕ characteristic of the meminductor emulator for different values of V_{offset}.

5. Conclusions.

In this communication the feasibility of a modified version of the Riordan gyrator to emulate floating meminductive systems has been demonstrated. The circuit proposed has been firstly described theoretically, from the modifications on the classical Riordan gyrator to its connection with the constitutive equations of flux-controlled meminductors. The theoretical approach has been supported with SPICE simulations using different inputs signals and frequencies for a simple two-states meminductor implementation as well as for a meminductor-based low-pass filter. Finally, a breadboard-level implementation of a continuous states meminductor demonstrates the simplicity, practicality and versatility of the emulator proposed.

Declaration of Competing Interest

The authors declare no conflict of interest.

Acknowledgments

This work was supported by the Spanish Ministry of Education, Culture, and Sport (MECD)/FEDER-EU through the grant FPU16/01451 and the project TEC2017-89955-P.

References

[1] L. Chua, "Memristor-The missing circuit element," *IEEE Transactions on Circuit Theory*, vol. 18, no. 5, pp. 507–519, Sep. 1971, doi: 10.1109/TCT.1971.1083337.

[2] D. B. Strukov, G. S. Snider, D. R. Stewart, and R. S. Williams, “The missing memristor found,” *Nature*, vol. 453, no. 7191, Art. no. 7191, May 2008, doi: 10.1038/nature06932.

[3] P. 01 M. 2008 | 15:57 GMT, “The Mysterious Memristor - IEEE Spectrum,” *IEEE Spectrum: Technology, Engineering, and Science News*. https://spectrum.ieee.org/semiconductors/design/the-mysterious-memristor (accessed Oct. 26, 2020).

[4] R. C. Johnson, “EETimes - Will memristors prove irresistible? -,” *EETimes*, Sep. 01, 2008. https://www.eetimes.com/will-memristors-prove-irresistible-2/ (accessed Oct. 26, 2020).

[5] M. D. Ventra, Y. V. Pershin, and L. O. Chua, “Putting Memory Into Circuit Elements: Memristors, Memcapacitors, and Meminductors [Point of View],” *Proceedings of the IEEE*, vol. 97, no. 8, pp. 1371–1372, Aug. 2009, doi: 10.1109/JPROC.2009.2022882.

[6] M. Di Ventra, Y. V. Pershin, and L. O. Chua, “Circuit Elements With Memory: Memristors, Memcapacitors, and Meminductors,” *Proceedings of the IEEE*, vol. 97, no. 10, pp. 1717–1724, Oct. 2009, doi: 10.1109/JPROC.2009.2021077.

[7] Y. V. Pershin and M. Di Ventra, “Neuromorphic, Digital, and Quantum Computation With Memory Circuit Elements,” *Proceedings of the IEEE*, vol. 100, no. 6, pp. 2071–2080, Jun. 2012, doi: 10.1109/JPROC.2011.2166369.

[8] C. Chen, H. Bao, M. Chen, Q. Xu, and B. Bao, “Non-ideal memristor synapse-coupled bi-neuron Hopfield neural network: Numerical simulations and breadboard experiments,” *AEU - International Journal of Electronics and*

Communications, vol. 111, p. 152894, Nov. 2019, doi: 10.1016/j.aeue.2019.152894.

[9] S. Kvatinsky *et al.*, “MAGIC—Memristor-Aided Logic,” *IEEE Transactions on Circuits and Systems II: Express Briefs*, vol. 61, no. 11, pp. 895–899, Nov. 2014, doi: 10.1109/TCSII.2014.2357292.

[10] S. Kvatinsky, N. Wald, G. Satat, A. Kolodny, U. C. Weiser, and E. G. Friedman, “MRL — Memristor Ratioed Logic,” in *2012 13th International Workshop on Cellular Nanoscale Networks and their Applications*, Aug. 2012, pp. 1–6, doi: 10.1109/CNNA.2012.6331426.

[11] N. Yang, C. Yang, Y. YU, X. LU, L. Wang, and T. Nyima, “Study on Acttive Filter Based on Memristor and Memcapacitor,” in *2018 Fifteenth International Conference on Wireless and Optical Communications Networks (WOCN)*, Feb. 2018, pp. 1–4, doi: 10.1109/WOCN.2018.8556125.

[12] H. Gan, D. Yu, D. Li, and H. Cheng, “Binary memcapacitor based first-order active filter,” *Circuit World*, vol. 46, no. 2, pp. 117–124, Jan. 2020, doi: 10.1108/CW-06-2019-0061.

[13] M. Wang, Y. Yu, N. Yang, C. Yang, and H. Ma, “New band-pass and band-stop filters with three memory devices,” in *2019 14th IEEE Conference on Industrial Electronics and Applications (ICIEA)*, Jun. 2019, pp. 1985–1989, doi: 10.1109/ICIEA.2019.8834352.

[14] Q. Zhao, C. Wang, and X. Zhang, “A universal emulator for memristor, memcapacitor, and meminductor and its chaotic circuit,” *Chaos*, vol. 29, no. 1, p. 013141, Jan. 2019, doi: 10.1063/1.5081076.

[15] F. Yuan and Y. Li, “A chaotic circuit constructed by a memristor, a memcapacitor and a meminductor,” *Chaos*, vol. 29, no. 10, p. 101101, Oct. 2019, doi: 10.1063/1.5125673.

[16] F. Yuan, G. Wang, and X. Wang, “Chaotic oscillator containing memcapacitor and meminductor and its dimensionality reduction analysis,” *Chaos*, vol. 27, no. 3, p. 033103, Mar. 2017, doi: 10.1063/1.4975825.

[17] X. Wang, J. Yu, C. Jin, H. H. C. Iu, and S. Yu, “Chaotic oscillator based on memcapacitor and meminductor,” *Nonlinear Dyn*, vol. 96, no. 1, pp. 161–173, Apr. 2019, doi: 10.1007/s11071-019-04781-5.

[18] M. Yildirim and F. Kacar, “Chaotic circuit with OTA based memristor on image cryptology,” *AEU - International Journal of Electronics and Communications*, vol. 127, p. 153490, Dec. 2020, doi: 10.1016/j.aeue.2020.153490.

[19] E. Gale, “TiO2-based memristors and ReRAM: materials, mechanisms and models (a review),” *Semicond. Sci. Technol.*, vol. 29, no. 10, p. 104004, Sep. 2014, doi: 10.1088/0268-1242/29/10/104004.

[20] F. J. Romero *et al.*, “Laser-Fabricated Reduced Graphene Oxide Memristors,” *Nanomaterials*, vol. 9, no. 6, Art. no. 6, Jun. 2019, doi: 10.3390/nano9060897.

[21] F. J. Romero *et al.*, “Resistive Switching in Graphene Oxide,” *Front. Mater.*, vol. 7, 2020, doi: 10.3389/fmats.2020.00017.

[22] D. Biolek and V. Biolkova, “Mutator for transforming memristor into memcapacitor,” *Electronics Letters*, vol. 46, no. 21, pp. 1428–1429, Oct. 2010, doi: 10.1049/el.2010.2309.

[23] M. Pd. Sah, R. K. Budhathoki, C. Yang, and H. Kim, “Expandable circuits of mutator-based memcapacitor emulator,” *Int. J. Bifurcation Chaos*, vol. 23, no. 05, p. 1330017, May 2013, doi: 10.1142/S0218127413300176.

[24] X. Y. Wang, A. L. Fitch, H. H. C. Iu, and W. G. Qi, “Design of a memcapacitor emulator based on a memristor,” *Physics Letters A*, vol. 376, no. 4, pp. 394–399, Jan. 2012, doi: 10.1016/j.physleta.2011.11.012.

[25] D. S. Yu, Y. Liang, H. Chen, and H. H. C. Iu, “Design of a Practical Memcapacitor Emulator Without Grounded Restriction,” *IEEE Transactions on Circuits and Systems II: Express Briefs*, vol. 60, no. 4, pp. 207–211, Apr. 2013, doi: 10.1109/TCSII.2013.2240879.

[26] Y. V. Pershin and M. D. Ventra, “Memristive circuits simulate memcapacitors and meminductors,” *Electronics Letters*, vol. 46, no. 7, pp. 517–518, Apr. 2010, doi: 10.1049/el.2010.2830.

[27] D.-S. Yu, Y. Liang, H. H. C. Iu, and Y.-H. Hu, “Mutator for transferring a memristor emulator into meminductive and memcapacitive circuits,” *Chinese Phys. B*, vol. 23, no. 7, p. 070702, Jul. 2014, doi: 10.1088/1674-1056/23/7/070702.

[28] S.-F. Wang, “The gyrator for transforming nano memristor into meminductor,” *Circuit World*, vol. 42, no. 4, pp. 197–200, Jan. 2016, doi: 10.1108/CW-01-2016-0002.

[29] F. Yuan, Y. Jin, and Y. Li, “Self-reproducing chaos and bursting oscillation analysis in a meminductor-based conservative system,” *Chaos*, vol. 30, no. 5, p. 053127, May 2020, doi: 10.1063/5.0008313.

[30] F. J. Romero *et al.*, “Memcapacitor emulator based on the Miller effect,” *International Journal of Circuit Theory and Applications*, vol. 47, no. 4, pp. 572–579, 2019, doi: 10.1002/cta.2604.

[31] M. E. Fouda and A. G. Radwan, “Charge controlled memristor-less memcapacitor emulator,” *Electronics Letters*, vol. 48, no. 23, pp. 1454–1455, Nov. 2012, doi: 10.1049/el.2012.3151.

[32] Yan L., Dong-Sheng Y., and Hao C., “A novel meminductor emulator based on analog circuits,” *wlxb*, vol. 62, no. 15, pp. 158501–158501, Aug. 2013, doi: 10.7498/aps.62.158501.

[33] M. Konal and F. Kacar, “Electronically tunable meminductor based on OTA,” *AEU - International Journal of Electronics and Communications*, vol. 126, p. 153391, Nov. 2020, doi: 10.1016/j.aeue.2020.153391.

[34] M. E. Fouda and A. G. Radwan, “Memristor-less current- and voltage-controlled meminductor emulators,” in *2014 21st IEEE International Conference on Electronics, Circuits and Systems (ICECS)*, Dec. 2014, pp. 279–282, doi: 10.1109/ICECS.2014.7049976.

[35] M. E. Fouda and A. G. Radwan, “Meminductor Response Under Periodic Current Excitations,” *Circuits Syst Signal Process*, vol. 33, no. 5, pp. 1573–1583, May 2014, doi: 10.1007/s00034-013-9708-y.

[36] F. J. Romero, M. Escudero, A. Medina-Garcia, D. P. Morales, and N. Rodriguez, “Meminductor Emulator Based on a Modified Antoniou’s Gyrator Circuit,” *Electronics*, vol. 9, no. 9, Art. no. 9, Sep. 2020, doi: 10.3390/electronics9091407.

[37] R. H. S. Riordan, “Simulated inductors using differential amplifiers,” *Electronics Letters*, vol. 3, no. 2, pp. 50–51, Feb. 1967, doi: 10.1049/el:19670039.

[38] R. Senani, D. R. Bhaskar, A. K. Singh, and V. K. Singh, “Simulation of Inductors and Other Types of Impedances Using CFOAs,” in *Current Feedback Operational Amplifiers and Their Applications*, R. Senani, D. R. Bhaskar, A. K. Singh, and V. K. Singh, Eds. New York, NY: Springer, 2013, pp. 49–80.

[39] D. V. Kamath, “Overview of OPAMP and OTA based Integrators,” *International Journal of Innovative Research in Electrical, Electronics, Instrumentation and Control Engineering*, vol. 3, no. 9, pp. 74–79, Sep. 2015, doi: 10.17148/IJIREEICE.2015.3915.

[40] X.-Y. Wang, A. L. Fitch, H. H. C. Iu, V. Sreeram, and W.-G. Qi, “Implementation of an analogue model of a memristor based on a light-dependent resistor,” *Chinese Phys. B*, vol. 21, no. 10, p. 108501, Oct. 2012, doi: 10.1088/1674-1056/21/10/108501.